Received: 16 June 2022 | Accepted: 3 January 2023

DOI: 10.1111/srt.13279

ORIGINAL ARTICLE

WILEY

Noninvasive imaging exploration of phacomatosis pigmentokeratotica using high-frequency ultrasound and optical coherence tomography: Can biopsy of PPK patients be avoided?

Jenna Lee[1] | Juliana Benavides[2] | Rayyan Manwar[2] | Carolina Puyana[1] | Julia May[1] | Maria Tsoukas[1] | Kamran Avanaki[1,2]

[1]Dermatology Department, College of Medicine, University of Illinois—Chicago, Chicago, Illinois

[2]Richard and Loan Hill Biomedical Engineering Department, College of Engineering and Medicine, University of Illinois—Chicago, Chicago, Illinois

Correspondence
Kamran Avanaki, Dermatology Department, University of Illinois—Chicago, Chicago, IL 60607.
Email: avanaki@uic.edu

Abstract

Background: Phacomatosis pigmentokeratotica (PPK) is a distinct and rare type of epidermal nevus syndrome characterized by coexisting nonepidermolytic organoid sebaceous nevus (SN) with one or more speckled lentiginous nevi (SLN). Atypical nevi including compound Spitz and compound dysplastic may manifest within regions of SLN. Patients with PPK, or similar atypical nevus syndromes, may be subject to a significant lifetime number of biopsies, leading to pain, scarring, anxiety, financial burden, and decreased quality of life. The current literature includes case reports, genetics, and associated extracutaneous symptoms of PPK, but use of noninvasive imaging techniques have not been explored. We aim to investigate the value of high-frequency ultrasound (HFUS) and optical coherence tomography (OCT) in discriminating morphological features of pigmented lesions and nevus sebaceous within one patient with PPK.

Materials and methods: Two modalities, (1) HFUS imaging, based on acoustic properties and (2) OCT imaging, based on optical properties, were used to image a patient with PPK. Benign pigmented lesions, which may raise clinical suspicion for significant atypia, and nevus sebaceous, were selected on different areas of the body to be studied.

Results: Five pigmented lesions and one area of nevus sebaceous were imaged and analyzed for noninvasive features. Distinct patterns of hypoechoic features were seen on HFUS and OCT.

Conclusion: HFUS provides a deep view of the tissue, with ability to differentiate gross structures beneath the skin. OCT provides a smaller penetration depth and a

higher resolution. We have described noninvasive features of atypical nevi and nevus sebaceous on HFUS and OCT, which indicate benign etiology.

KEYWORDS
atypical nevi, epidermal nevus syndrome, melanoma, noninvasive imaging, optical coherence tomography, phacomatosis pigmentokeratotica, skin cancer, ultrasound

1 | INTRODUCTION

Phacomatosis pigmentokeratotica (PPK), first described by Rudolph Happle in 1996, is a distinct and rare type of epidermal nevus syndrome characterized by coexisting nevus sebaceous and one or more speckled lentiginous nevi (SLN).[1] Nevus sebaceous (NS), otherwise known as nevus sebaceous of Jadassohn,[2] is a congenital malformation that includes hamartomas of the pilosebaceous follicular unit. At birth, NS may appear as a yellow, solitary, smooth well-circumscribed plaque with an oval or linear pattern. If they appear as multiple lesions, they may arise along Blaschko lines of embryonal development. During puberty, NS becomes more pronounced with verrucous or mammillated texture changes secondary to developing hormonal differences. NS is commonly found on the scalp, forehead, face, or neck.[2] The coexisting SLN, otherwise known as nevus spilus, is described as larger café-au-lait macules with numerous smaller superimposed darker black or brown melanocytic proliferations.[3] The superimposed lesions may appear in wide ranges of sizes ranging from a 1 to 100 mm.[3–5] Both NS and SLN are commonly asymptomatic. Epidemiologically, PPK is more commonly present in males with a ratio of 12:5.[6] Only 30 cases of PPK globally have been reported in literature.[7] Due to the rarity of PPK, statistical data has been inconclusive for incidence and prevalence of this condition in the United States.

The genetic cause of PPK is a single dominant heterozygous activating HRAS mutation, which leads to the two different types of nevi.[8] The melanocytes within the speckled lentiginous nevi of PPK carry the causal mosaic HRAS c.37G > A mutation. Groesser et al. hypothesized that this mutation affects a multipotent progenitor cell, which could then cause both cutaneous and extracutaneous manifestations seen in PPK.[8] For example, a mutation in an ectodermal progenitor cell may cause anomalies such as epidermal nevi and central nervous system defects; a mesodermal progenitor cell would give rise to vascular and skeletal anomalies; and so forth. Groesser et al. also theorized that the mutation causing PPK has a temporal component, such that if the mutation occurred prior to neural crest differentiation, the ectodermal progenitor cell would affect both keratinocytes and melanocytes. Of note, Spitz nevi may also be found within speckled lentiginous nevi of PPK patients. Both HRAS c.37G > C and HRAS c.182A > G mutations have been found in Spitz nevi, further supporting HRAS as the causative genetic mutation involving PPK.[9]

As an epidermal nevus syndrome, PPK is associated with extracutaneous manifestations such as neurological, musculoskeletal, and ocular disorders. The associated neurological defects are typically ipsilateral and corresponding to the limbs that are affected cutaneously. Neurological abnormalities most commonly associated with PPK are hemiatrophy, hemiparesis, sensory neuropathy, motor neuropathy, hyperhidrosis, cutaneous dysesthesia, seizure, and muscular weakness.[1,4,10] Other reported extracutaneous features include hypophosphatemic vitamin D-resistant rickets, kyphosis, scoliosis, and ocular involvement such as ptosis, strabismus, and congenital glaucoma. Associated systemic conditions also include three reported cases of arterial hypertension, as well vascular, renal, and urologic defects.[1,4,9,10] Within the sebaceous nevus areas, development of secondary neoplasms may occur. Benign neoplasms arising in this area may include, trichoblastoma, trichilemmoma, and hidradenoma with syringocystadenoma papilliferum being the most common at a rate of approximately 10%–20%.[11,12] Additionally, the most common malignant neoplasm arising in this area is basal cell carcinoma, with a frequency of ranging from 6.5% to 22%.[10,12,13] Rarely, squamous cell carcinoma may develop.[12] Within regions of the SLN particularly, secondary cutaneous manifestations are rare, though cases of malignant melanoma have been reported.[6,10]

Schimmelpenning syndrome[10] presents similarly to PPK, as both syndromes are caused by a common HRAS mosaic mutation and are defined by associated nevus sebaceous components along lines of Blaschko. Schimmelpenning syndrome however differs in associated extracutaneous involvement, such as coloboma and lipodermoid of the conjunctiva.[10,14] Genetically, in Schimmelpenning syndrome, the mutated progenitor cell loses the ability to differentiate into melanocytes, whereas in PPK, mutated progenitor cells are able to differentiate into melanocytes and epithelial cells.[15] Of note patients with PPK have a higher propensity of developing a true basal cell carcinoma within nevus sebaceous lesions compared to patients with Schimmelpenning syndrome and of the general population.[4]

Currently, biopsy and histopathological examination is the standard used to diagnose concerning PPK lesions. Typical histology of different types of lesions on PPK patients are graphically depicted in Figure 1. On histology, increased pigmentation can be found at the basal layer of the epidermis of SLN lesions. There is also lentiginous epidermal hyperplasia present correlating clinically to the café-au-lait hyperpigmented background patch, similar to that of lentigo simplex. There are elongated rete ridges with scattered melanocytes and melanocytic proliferation at the dermal-epidermal junction (DEJ) and tips of rete ridges[16,17] (Figure 1A). The papular variant of SLN, most commonly associated with patients with PPK, consists of junctional, compound, and dermal melanocytic nevi unevenly distributed within the light-brown macular patch.[17] Junctional melanocytic nevi (Figure 1B) show discrete nests of melanocytes at the DEJ with common melanocytic nests densities at

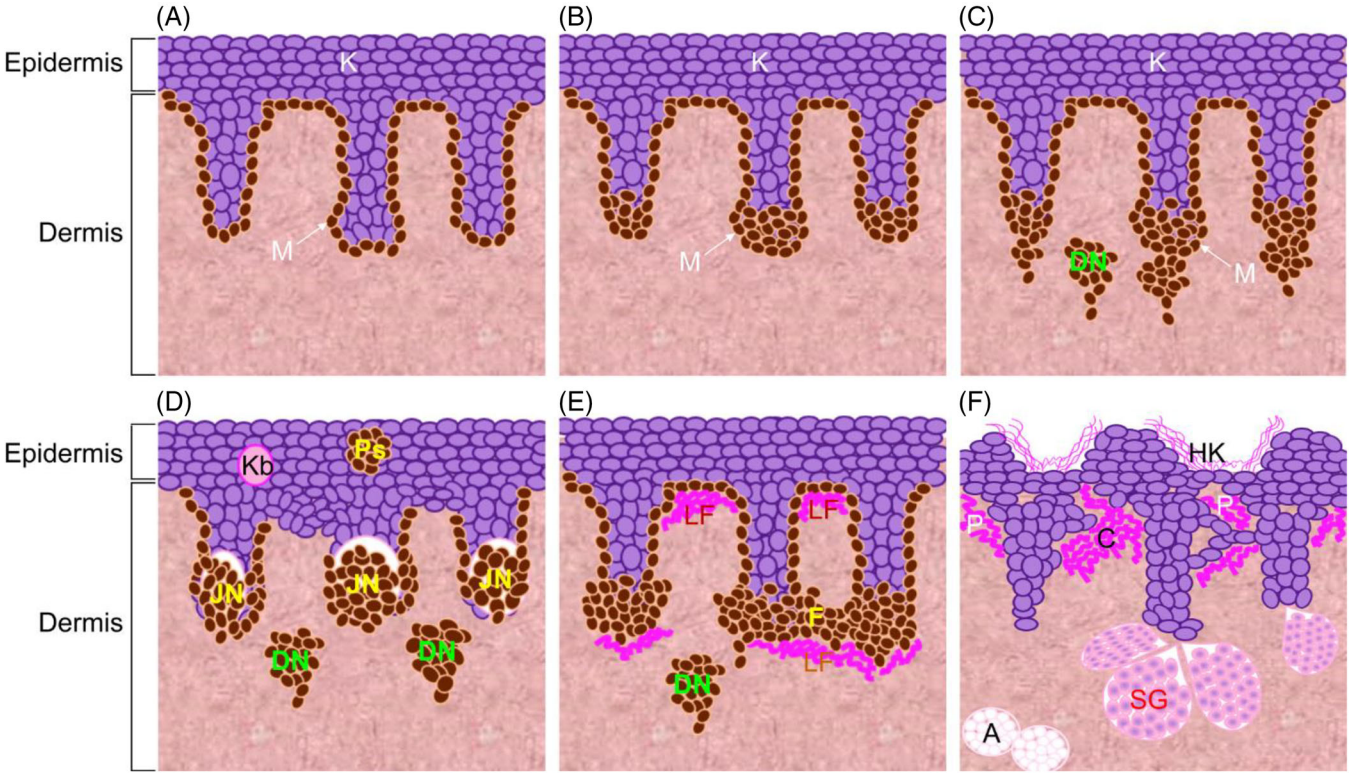

FIGURE 1 Histology graphic of different types of lesions seen in Phacomatosis pigmentokeratotica (PPK). **(A)** Speckled lentiginous nevus (SLN) demonstrates normal epidermis with keratinocytes (K) and melanocyte (M) proliferation along the basal layer of elongated rete ridges in the epidermis. **(B)** Junctional nevus demonstrates normal epidermis with keratinocytes (K), basal layer melanocytes (M), and proliferative melanocytic nests at the tips of elongated rete ridges. The nests do not extend beyond the basal layer. **(C)** Compound nevus demonstrates normal epidermal keratinocytes (K) and lentiginous melanocytic proliferation with extension of melanocytes (M) beyond the basal layer of the epidermis. Nests of melanocytes are present within the dermis (DN). **(D)** Compound Spitz nevus demonstrates epidermal acanthosis, large junctional nests (JN) at tips of elongated rete ridges, and presence of melanocytic nests in the dermis (DN). Note the clefting artifact within JN. Kamino bodies (Kb) present in the epidermis are indicative of benign etiology of the nevus. Pagetoid spread (Ps) of melanocytic nests or single melanocytes extending toward the surface of the epidermis. **(E)** Compound dysplastic nevus demonstrates elongated rete ridges with fusion of melanocytic nests (F). Melanocytes extend beyond the basal layer into the dermis (DN). Shouldering is present when junctional component extends to three rete ridges beyond the dermal component. Concentric papillary dermal fibrosis or lamellar fibroplasia (LF) is present. **(F)** Nevus sebaceous demonstrates acanthosis, hyperkeratosis (HK), and epithelial papillomatosis (P). Histology indicates hamartomas of large sebaceous glands (SG), papillary collagen deposition (C), and ectopic apocrine glands (A). K: keratinocytes, M: melanocytes, DN: melanocytic nests in dermis, JN: junctional nest, Kb: kamino bodies, Ps: pagetoid spread, F: fusion of melanocytic nests, LF: lamellar fibroplasia, HK: hyperkeratosis, P: epithelial papillomatosis, SG: sebaceous glands, C: collagen deposition, A: ectopic apocrine glands.

rete ridges.[18] Compound nevi (Figure 1C) differ from junctional nevi by the presentation of nests of uniform melanocytes in both the epidermis and dermis. Compound nevi are occasionally raised, dome-shaped, and deeply pigmented. Marked hyperkeratosis and acanthosis may also be present. Like junctional nevi, junctional components have melanocytic nests (JN) lining the basal layer of the epidermis. The dermal component may consist of large dermal melanocytic nests (DN) that are organized in a linear distribution. Melanocytes are small with regular nuclei, scant cytoplasm, and normal maturation. Nevus melanocytic maturation refers to the gradual change of superficial melanocytic nest clusters into single file melanocytes with descent into the dermis. Typical maturation differentiates benign pigmented lesions from malignant lesions, which lack this pattern.[19,20]

Compound Spitz nevi (Figure 1D) and compound dysplastic nevi (Figure 1E) are two variants that can be found in PPK. Spitz nevi contain large, occasionally spindle-shaped, clefted, junctional melanocytic nests. Here, melanocytes have abundant pale pink or gray cytoplasm with large round nuclei and prominent central nucleoli. Although these may resemble a melanoma, the presence of benign determinants support the etiology of the lesion as "Spitzoid." Benign determinants of Spitz nevi include pagetoid spread (Ps) of melanocytic nests or single melanocytes and the presence of kamino bodies (Kb), large, dull-pink trapped basement membrane components that stain similarly to type IV collagen.[21] At low power, Spitz nevi are well circumscribed with nests ending abruptly at the periphery of the lesion, all of which are commonly absent in melanoma.[21,22] Compound dysplastic nevi are characterized by horizontally arranged melanocytic nests at the DEJ with extension of at least three rete ridges beyond the dermis. Bridging of nests between adjacent rete ridges with scattered singular melanocytes can be seen. In dysplastic

nevi, concentric papillary dermal fibrosis, lamellar fibroplasia (LF), and inflammatory infiltrate occur in attempt to wall off the downward proliferation of melanocytes.[23] Similar to Spitz nevi, dysplastic nevi have melanocyte nuclear enlargement, hyperchromasia, and prominent nucleoli.[24]

On the other hand, histology of NS (Figure 1F) reveals increased epidermal acanthosis and papillomatosis (P). During puberty, sebaceous glands (SG) become more prominent with increased number of sebaceous lobules and malformed ducts. Hair follicles on NS are immature terminal vellus hairs instead of terminal hairs. Buds of follicular germinative cells may be found at the DEJ.[25] The sebaceous glands are also unusually high in the dermis. Occasionally, ectopic apocrine glands (A) or eccrine hyperplasia may also be present.[2]

Patients with PPK and atypical nevus syndromes may have numerous pigmented lesions, which may fulfill the ABCDE checklist, increasing suspicion for melanoma. Dermoscopy is most commonly used to evaluate the lesion by visualizing subsurface colors, structures, and patterns; however, it is highly operator dependent. Histopathological examination via biopsy is the current gold standard in the diagnosis of melanoma; this is not only costly but also time consuming. Patients with PPK may require numerous invasive procedures over the course of their lifetime, leading to extensive morbidity and decreased quality of life. Patients are left with pain, scarring, and anxiety.

To avoid such variability in visual inspection and unnecessary biopsies, multiple noninvasive imaging technologies have been developed to characterize features of pigmented lesions below the surface of the skin. High-frequency ultrasound (HFUS) and optical coherence tomography (OCT) have proven to be promising technologies that may help in identifying atypical lesion characteristics below the surface of the skin. The premises of these imaging modalities are dependent on the lesion's cellular and structural acoustic and optical properties respectively, including scatter, absorption, and reflection.[26] HFUS creates images (depth < 5 cm) using high-frequency ultrasound waves (frequency > 10 MHz) that reflect off structures with different acoustic impedances. The transducer is a handheld probe containing several elements made of piezoelectric crystals, which are stimulated by an electric voltage, generating millions of acoustic sound waves. The ultrasound waves are transmitted from the transducer into the tissue, reflected back to the transducer, then converted back to electrical energy, and interpreted by computer software. HFUS has been used to visualize skin thickness, neoplasms, tumor thickness, and tumor depth.[27,28] HFUS has been reported to confirm dermatologic diagnoses (82%) and has aided in the revision of diagnoses (17%), demonstrating its value in dermatology.[29] HFUS has been most commonly used in the identification and diagnosis of basal cell carcinoma and squamous cell carcinoma margins; however, discrimination of benign pigmented lesions from malignant has remained challenging. Still, HFUS has proven efficacy in observing melanoma tumor thickness, vascularity, shape irregularity, and dermal invasion.[30] Alternatively, OCT uses a near-infrared low coherence light source, which is directed to tissue under examination. The delay in backscattered light, which reflects off microstructures, depicts different depths of light reflectance. Michelson interferometry[30] is used to measure the reflected light by comparing it to a known reference to that of the specimen. The incident light beam scans the tissue transversely as the backscattered profile at each position, allowing a real-time cross-sectional view of the skin.[30] OCT has been widely used to visualize nonmelanoma skin cancers and melanomas for diagnosis and tumor margin delineation, as well as a disease progression in inflammatory, infectious, and vascular etiologies.[31] Compared to HFUS, OCT has a smaller penetration depth of 1–2 mm with a field of view of 6 mm. However, its higher resolution of less than 10 μm provides improved visualization of tissue microstructures and architectural changes.

In this study, we utilized three noninvasive imaging tools (dermoscopy, HFUS, and OCT) to characterize various lesions on a patient with PPK. We then compared the corresponding images of benign nevi and nevus sebaceous, taken by each modality. Our goal is to discern whether visualizing noninvasive biomarkers demonstrated on imaging could be used as a diagnostic aid in the determination of benign versus malignant etiology and if implementing this multimodality approach may be enough to forego biopsy.

2 | MATERIALS AND METHODS

All imaging procedures and experimental protocols were approved and carried out based on guidelines of the Institutional Review Board of University of Illinois at Chicago College of Medicine (IRB #2021-0249). Informed consent was obtained by the subject prior to enrollment in the study. We investigate a female patient born to healthy nonconsanguineous parents. Family history is unremarkable. She presented with a sebaceous nevus on her right lateral neck, which extends midline anteriorly and chest distally. She had numerous SLN of the papulosa variant, in a checkerboard pattern involving both sides of the face, left and predominantly right shoulders, right upper back, right upper chest, lower back, and right lower extremity. Retrospective pathology reports dated from the patient's birth were analyzed. Previous biopsies of pigmented lesions include compound dysplastic nevi and compound Spitz nevi. The patient has also had areas of her scalp, right neck, and chest biopsied with diagnosis of nevus sebaceous. Past excised lesions also include syringocystadenoma papilliform and trichoblastoma. She has numerous similar morphological manifestations of Spitz nevi, which were described as occasionally pruritic, pink, dome shaped, oval nevi with central blue-white veil globules. Extracutaneous manifestations consist of primarily neurological and skeletal abnormalities, which involve right sided upper extremity and lower extremity hemiatrophy as well as right sided muscular weakness. She was born with a limb length discrepancy of 3 cm of the right lower extremity. Her history is significant for right sided bone abnormalities involving the right hemipelvis, right femur, and right tibia consistent with a variant of fibrous dysplasia, meloerostosis, and nonossifying fibromas. Past surgical history includes a significant number of biopsies of pigmented lesions and left knee growth plate removed in 2007. Due to continued limb length discrepancy of 2.5 cm and persistent pain due to significant stress fracture of the right tibia, an intermedullary nail was placed to protect the right tibia in 2017. The concomitant limb length discrepancy was

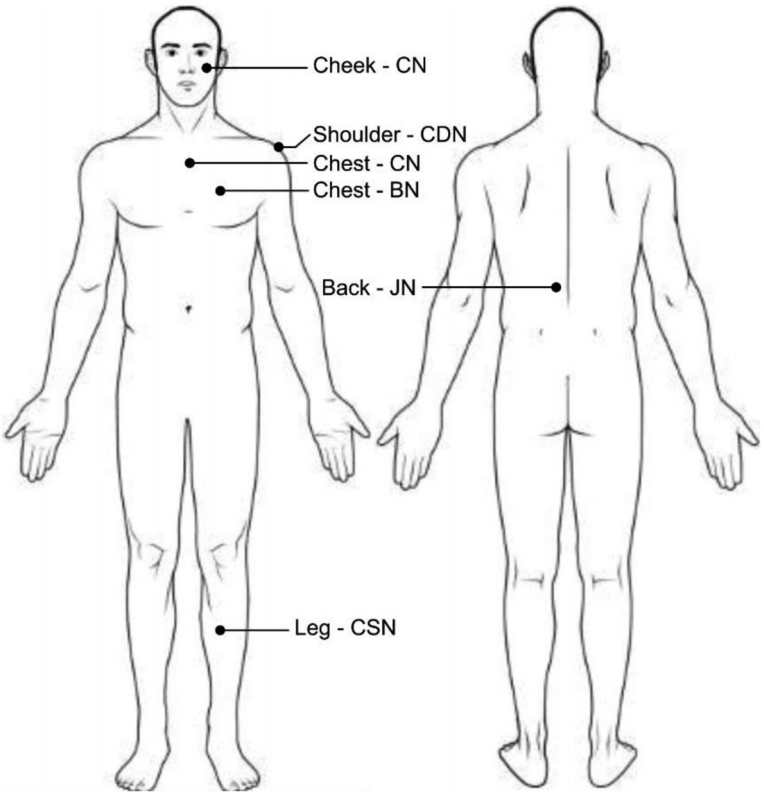

FIGURE 2 Map of lesions examined on the patient. NS: nevus sebaceous, BN: benign nevus, CN: compound nevus, CDN: compound dysplastic nevus, JN: junctional nevus, CSN: compound Spitz nevus.

addressed by left femur osteoplasty and shortening with placement of intermedullary nail for stabilization during the same procedure.

Five pigmented lesions on the left cheek, right chest, right shoulder, midline lower back, and right lower leg, and one area of nevus sebaceous on the chest were evaluated with dermoscopy, HFUS, and OCT (Figure 2). The pigmented lesions selected for this study have atypical morphological features, size > 5 mm, irregular colors and borders, and lesions that are flat or raised. All pigmented lesions were located within areas of the SLN. For the purposes of this study, excision was not performed as these lesions were deemed clinically benign related to her diagnosis of PPK. Once the lesion was identified, an image was taken with an iPhone XS (Apple Inc.), with a dermoscopy attachment (DermLite DL4N) in a polarized light setting with 90% isopropyl alcohol as a medium.

For HFUS image acquisition, we used VisualSonics Vevo 2100 (FujiFilm. VisualSonics Inc., Toronto, ON, Canada) equipped with a MS-550D (VisualSonics) linear array transducer of 256 elements. The transducer has a central frequency of 40.0 MHz (bandwidth: 22–55 MHz), an axial resolution of 40 μm, and a lateral resolution of 90 μm. The probe had the ability to image 18 mm in width and 10 mm in depth. A one-dimensional line graph called A-line was generated by each element and combined (using Vevo 2100) to produce B-mode images (cross-sectional images). Echogenicity or varying signal intensities on the B-mode images reflect specific characteristics of tissue. Hyperechoic or brighter regions represent abrupt increase in tissue density. Hypoechoic or darker regions represent decrease or no change in tissue density.[32,33] The examination was performed by placing the probe perpendicular to the surface of each of the six lesions of interest and slowly moving the transducer over the lesion. The probe was placed directly to the center of the lesion, with the probe orientation parallel to the widest length of the lesion. For each lesion, a 5-s video with 300 frames of B-mode images per second was captured. From the video, a single image was selected as the best representation of the lesion. For coupling, ultrasound gel was applied to the lesion of interest.

The OCT used in this study was a multibeam, swept source system (Vivosight, Michelson Diagnostic Inc.) with a hand-held probe used for skin imaging. The light source consisted of a broadband laser with a central wavelength of 1305 ± 15 nm. The scanning area was 6 mm in width × 6 mm in length × 2 mm in depth. It had an axial resolution of 10 μm and a lateral resolution of 7.5 μm. The OCT image was created by the reflectivity profile or the change in reflectivity with depth. This reflectivity profile is called the axial scan (A-scan). To generate a cross-sectional image, or the B-scan, the OCT system combined several A-lines for each transverse position of an incident beam on imaging target.[34] The pigmented lesion of interest was identified and cleaned with an alcohol prep pad. Then, the OCT probe was applied perpendicular to the skin with orientation ensuring the center of the lesion would be imaged. 50 B-scan OCT images were collected per pigmented lesion of interest.

3 | RESULTS

The pigmented lesion on the left cheek was 8 mm × 10 mm (Figure 3). On dermoscopy, the lesion has central hyperpigmentation, large peripheral globules, pink-red peripheral erythema, and a peripheral

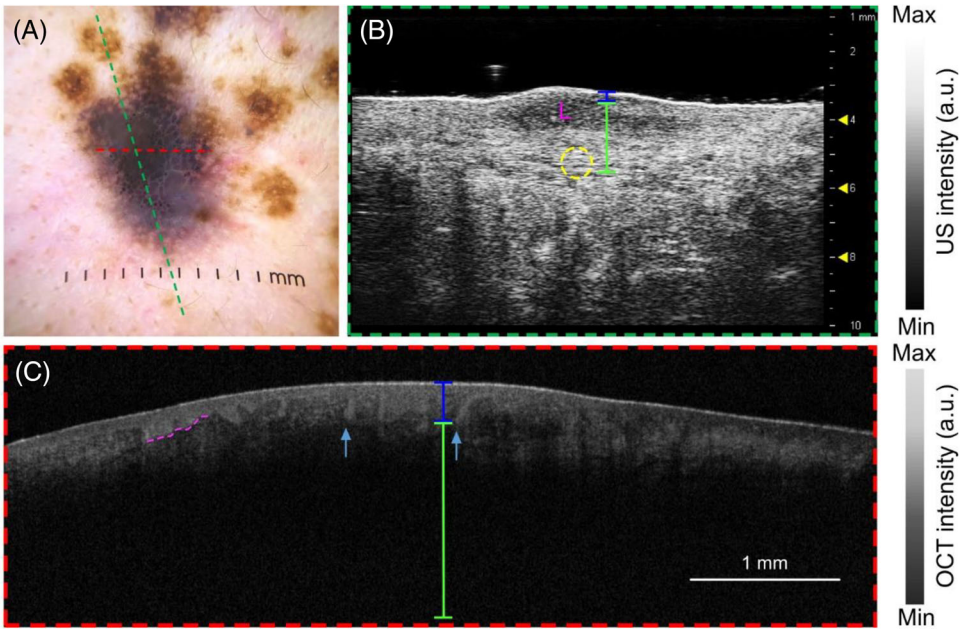

FIGURE 3 Compound nevus (CN) of phacomatosis pigmentokeratotica (PPK) on the left cheek. **(A)** Dermoscopy image of CN-cheek with central hyperpigmentation, large peripheral globules, and peripheral blue-white veil. Red dashed line—optical coherence tomography (OCT) probe field (6 mm). Green dashed line—high-frequency ultrasound (HFUS) probe field 16 mm. **(B)** HFUS image of the CN demonstrates a hypoechoic "straw hat sign" typical for CN. Areas of noise must be noted. L—lesion. Blue line—epidermal entry echo. Green line—dermis. Yellow dashed circle—focal areas of increased collagen surrounding CN. **(C)** OCT image of the CN-cheek. Blue line—epidermis. Green line—dermis. Pink dashed line—areas of fused and broadened rete ridges in the epidermis. Blue arrows—elongated rete ridges extending into papillary dermis.

blue-white veil (Figure 3A). The lesion has collisional components with neighboring smaller, symmetric, light brown junctional nevi. The HFUS image (Figure 3B) demonstrates an 8 mm wide and 1.5 mm deep hypoechoic area immediately below the epidermis/epidermal entrance signal (L: lesion). This darker signal pattern may be described as a "straw hat sign," indicative of a compound nevus.[18] The lesion extends deeper into the dermis with noticeable focal posterior signal intensity (yellow circle) immediately surrounding the hypoechoic area in a discoid-like shape. The bright signal intensity extends into the deep dermis and subcutis regions. On OCT image (Figure 3C), the epidermis is thickened. Elongated rete ridges, which extend into the papillary dermis (blue arrows), can be seen. In some areas, rete ridge fusion may be appreciated (pink dashed line).[34]

The pigmented lesion on the right chest was 5 mm × 7 mm (Figure 4). On dermoscopy, central black-brown globules, central whitish cast, and lighter brown peripheral reticular network are visualized (Figure 4A). The lesion demonstrates collision with three adjacent pigmented lesions. The HFUS image (Figure 4B) demonstrates a 5 mm wide, 0.5 mm depth, and hypoechoic lesion (L) immediately below the epidermal entry echo. The hypoechoic signal extends horizontally to the right of the hypoechoic lesion in Figure 4B, with 0.2 mm in depth, correlating to the adjacent colliding pigmented lesion. To the left of the hypoechoic lesion on HFUS, the hypoechoic line between the epidermis and dermis is much thinner, correlating to the pigmented lesion drop off to the background of lentiginous areas of SLN. The hypoechoic area is well demarcated from the brighter dermis directly below. The central part of the lesion extends into the dermis minimally without significant disruption of the dermis architecture. The subcutis (SC) and fascia (Fas) underlying the dermis can be well visualized. On OCT (Figure 4C), two distinctive morphological areas can be appreciated. The blue dashed line on the left in Figure 4C demonstrates elongated rete ridges extending into the papillary dermis. This correlates to the lesions peripheral reticular network (RN). The pattern fades into the area denoted by white dashed line. This part of the lesion demonstrates a loss of the DEJ signal intensity, which delineates epidermis from the dermis. The epidermis homogenously extends into the dermis in a disc-like fashion.

The pigmented lesion on the right shoulder was 7 mm × 9 mm (Figure 5). On dermoscopy, black-brown central hyperpigmentation with peripheral teared globules and blue-white veil are present with a pale brown lentiginous background (Figure 5A). The lesion demonstrates collision with two neighboring pigmented lesions on either side. The HFUS image (Figure 5B) demonstrates a 5.5 mm wide, 0.8 m depth, and hypoechoic lesion (L). The "straw-hat sign" is present indicating the compound nature of the nevus.[18] The hypoechoic lesion extends deeper toward the dermis and remains well demarcated from the dermis below. The darker signal thins out and extends laterally on either side of the lesion, correlating to the colliding pigmented lesions to the left and right, adjacent to the lesion of interest. Underlying the dermis, the subcutaneous tissue (SC) and fascia (Fas) can be appreciated. On OCT (Figure 5C), there is significant epidermal and dermal architectural disarray. Bright flame-shaped signal intensities arising from the dermis toward the epidermis can be noted, correlating with lamellar fibroplasia (orange arrows) seen in dysplastic nevi. Pathophysiologically, lamellar fibroplasia occurs in attempt to wall off proliferative

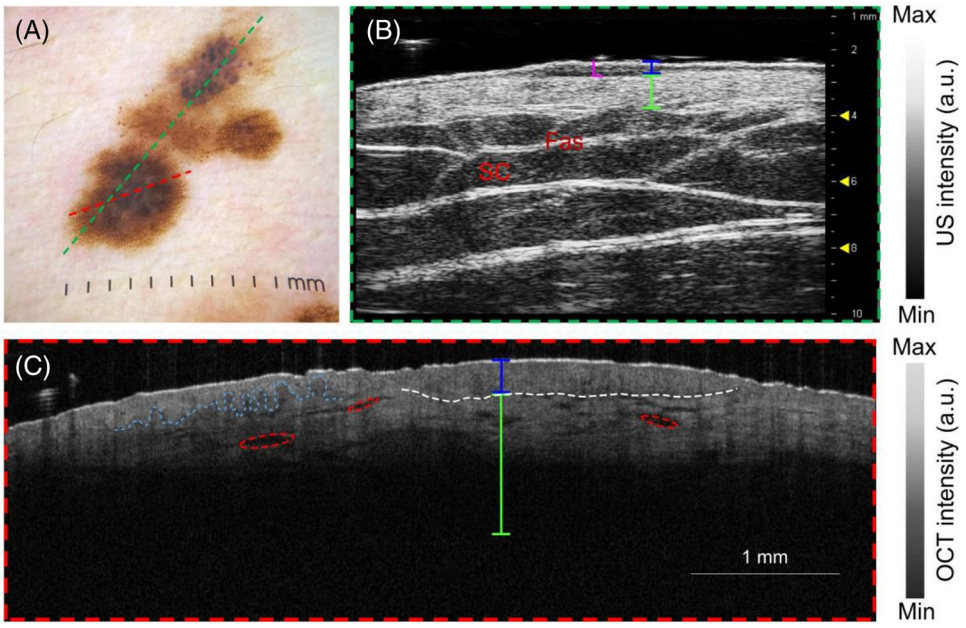

FIGURE 4 Compound nevus (CN) of phacomatosis pigmentokeratotica (PPK) on the chest. **(A)** Dermoscopy image of CN-chest with central black-brown globules are present with peripheral reticular network (RN). Red dashed line—optical coherence tomography (OCT) probe field (6 mm). Green dashed line—high-frequency ultrasound (HFUS) probe field 16 mm. **(B)** HFUS image of the CN-chest. L—lesion with hypoechoic "straw hat sign." Blue line—epidermal entry echo. Green line—dermis. SC—subcutis. Fas—fascia. **(C)** OCT image of the CN-chest. The epidermis blends homogenously into the dermis due to proliferation of melanocytic nests. Blue line—epidermis. Green line—dermis. Red dashed ovals—blood vessels. Blue dashed line—outlines the junctional portion of the CN, demonstrated by RN on dermoscopy. White dashed line—outlines the compound portion of the CN.

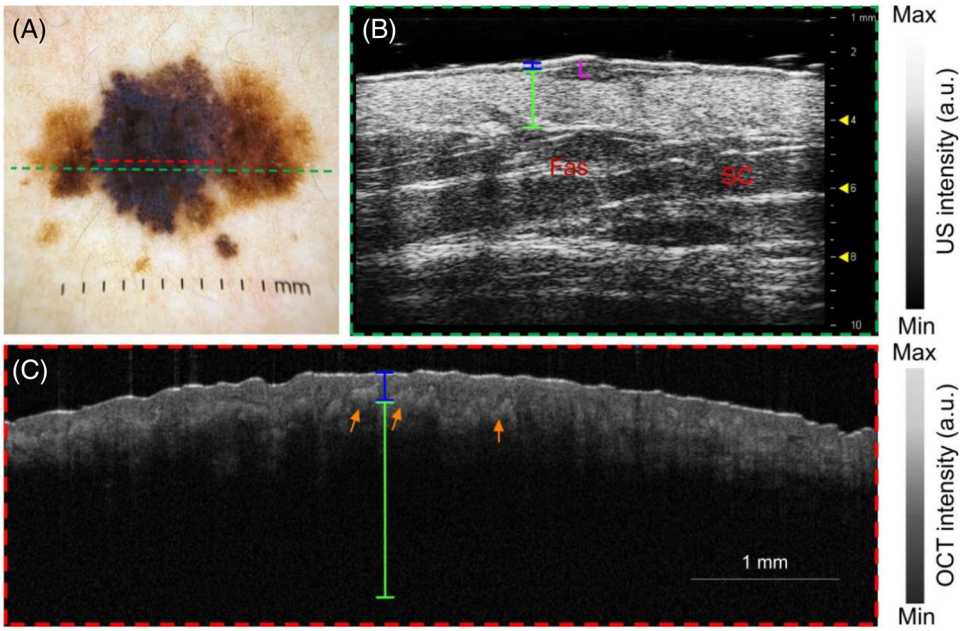

FIGURE 5 Compound dysplastic nevus (CDN) of phacomatosis pigmentokeratotica (PPK) on the shoulder. **(A)** Dermoscopy image of CDN-shoulder. Central hyperpigmentation with peripheral teared globules and blue-white veil are present. Red dashed line—optical coherence tomography (OCT) probe field (6 mm). Green dashed line—high-frequency ultrasound (HFUS) probe field 16 mm. **(B)** HFUS image of the CDN-shoulder. L—lesion. Blue line—epidermal entry echo. Green line—dermis. SC—subcutis. Fas—fascia. **(C)** OCT image of the CDN. Blue line—epidermis. Green line—dermis. Orange arrows—point to lamellar fibroplasia.

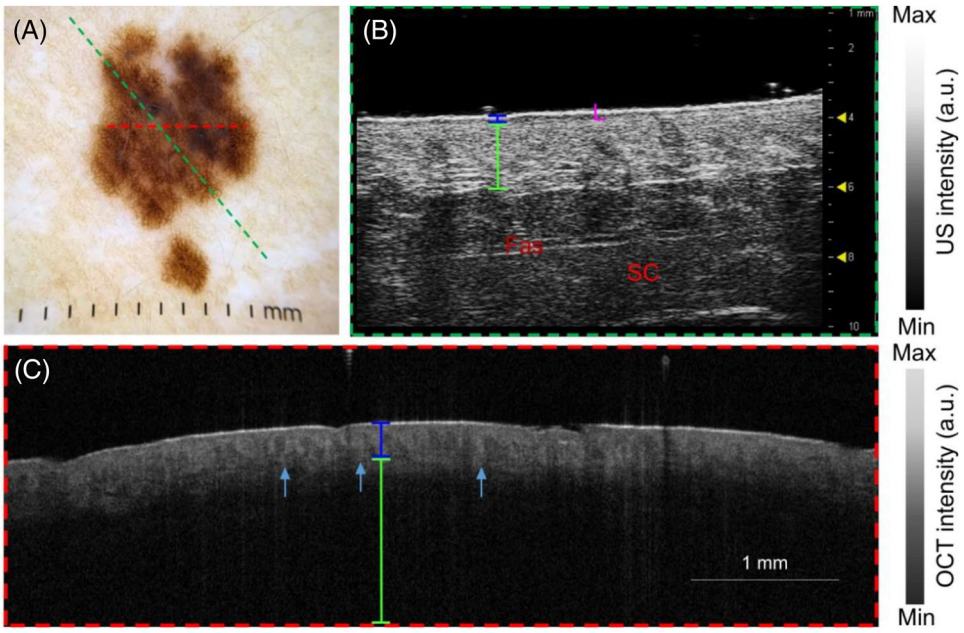

FIGURE 6 Junctional nevus (JN) of phacomatosis pigmentokeratotica (PPK) on the back. **(A)** Dermoscopy image of JN-back with light brown reticular network with scant areas of darker brown hyperpigmentation. Red dashed line—optical coherence tomography (OCT) probe field (6 mm). Green dashed line—high-frequency ultrasound (HFUS) probe field 16 mm. **(B)** HFUS image of the JN-back. L—lesion. Blue line—epidermal entry echo. Green line—dermis. SC—subcutis. Fas—fascia. "Strip-shaped" hypoechoic area is noted below the epidermis. **(C)** OCT image of the JN-back. Blue line—epidermis. Green line—dermis. Blue arrows—point to elongated rete ridges with lentiginous pattern.

melanocytes descending into the dermis.[23,24] Additionally, there is a lack of DEJ signal intensity, which does not clearly separate epidermis from dermis. The epidermis fades homogenously into the dermis below.

The pigmented lesion of the midline lower back was 8 mm × 9 mm (Figure 6). On dermoscopy, light brown reticular network with scant areas of darker brown hyperpigmentation is seen on a background of pale brown lentiginous patches (Figure 6A). The HFUS image (Figure 6B) demonstrates a thin 8 mm wide, 0.15 mm depth, and hypoechoic strip immediately below the epidermal entrance signal. The hypoechoic lesion (L) extends horizontally to either side but does not extend into the dermis below, correlating to the junctional nature of this pigmented lesion.[18] Throughout the image, the dermis remains architecturally intact without structural effacement. Underlying the dermis, the subcutaneous tissue (SC) and fascia (Fas) can be appreciated. On OCT image (Figure 6C), elongation of rete ridges into the papillary dermis is evident as well as rectification pattern of rete ridge (blue arrows).

The pigmented lesion on the right lower leg was 10 mm × 17 mm, slightly raised, and firm on palpation (Figure 7). On dermoscopy (Figure 7A), a pink, dome-shaped oval nevus with central blue-white veil globules and superimposed black-brown hyperpigmented densities is seen. The HFUS image (Figure 7B) demonstrates a 9 mm wide, 1.25 mm depth, and disc-shaped hypoechoic lesion below the epidermal entrance signal. There is a bright thin horizontal line intensity, which lays over the hypoechoic lesion and divides the epidermis from the dermis. The hypoechoic lesion is primarily located within the dermis, without clear demarcation from the surrounding tissue within the dermis. Surrounding the hypoechoic disc is a focal bright signal intensity correlating to increased dermal density. The subcutis and structures below the dermis remain intact. On OCT image (Figure 7C), epidermal thickness and density is increased demonstrated by the brighter signal intensity compared to other pigmented lesions in this study. Numerous elongated rete ridges are present (blue arrows), which extend into the papillary dermis. Areas of the lesion demonstrate rete ridge rectification indicating melanocytic nest rete ridge fusion, flattening (pink dashed line) of the epidermis followed by hyporeflective area below.[34]

The nevus sebaceous lesion was located on the chest (Figure 8). On dermoscopy (Figure 8A), firm yellow-tan globules aggregated in clusters on a lentiginous background with scattered collisional junctional nevi are present. The HFUS image (Figure 8B) demonstrates numerous hypoechoic areas underlying a thickened epidermal entrance signal. Epidermal thickening is observed. The hypoechoic globules are connected beneath the epidermis without septae in between them. The lesions extend very minimally into the dermis below without significant dermal architectural effacement. Within the dermis are oval hypoechoic areas (yellow arrows), which may indicate areas of sebaceous gland hyperplasia.[35] The dermis and subcutis below remain intact. On OCT image (Figure 8C), the epidermis is thickened with homogenous blending into the dermis, reflecting its acanthotic and hyperkeratotic nature. Within the dermis are numerous flame-shaped brighter signal intensities extending toward the epidermis, correlating to papillary dermis collagen deposition (yellow arrows). There are also vertical oval hypoechoic lesions (white arrows) with extension from the dermis to the surface of the epidermis, correlating with papillomatosis.[2] Sebaceous gland hyperplasia, which may be seen in the reticular dermis,

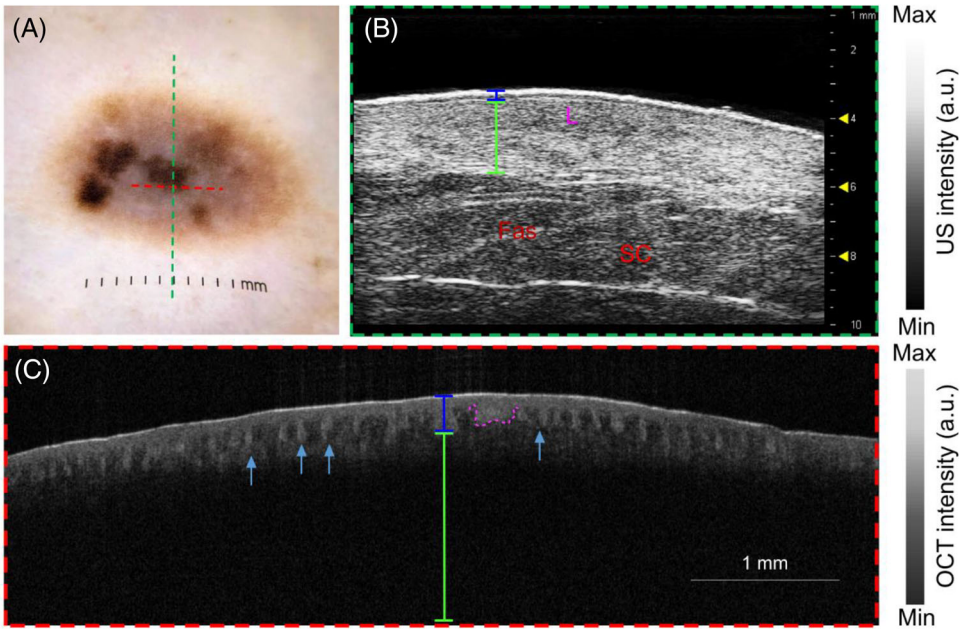

FIGURE 7 Compound Spitz nevus (CSN) of phacomatosis pigmentokeratotica (PPK) on the leg. **(A)** Dermoscopy image of CSN-leg with a pink, dome shaped, oval nevi with central blue-white veil globules and superimposed dark black-brown hyperpigmented densities. Red dashed line—optical coherence tomography (OCT) probe field (6 mm). Green dashed line—high-frequency ultrasound (HFUS) probe field 16 mm. **(B)** HFUS image of the CSN-leg. Epidermis is thickened. The lesion is ovoid and hypoechoic with extension into the dermis. L—lesion. Blue line—epidermal entry echo. Green line—dermis. SC—subcutis. Fas—fascia. **(C)** OCT image of the CSN-leg. Blue line—epidermis. Green line—dermis. Pink dashed line—fusion and broadening of rete ridges. Blue arrows—elongated rete ridges.

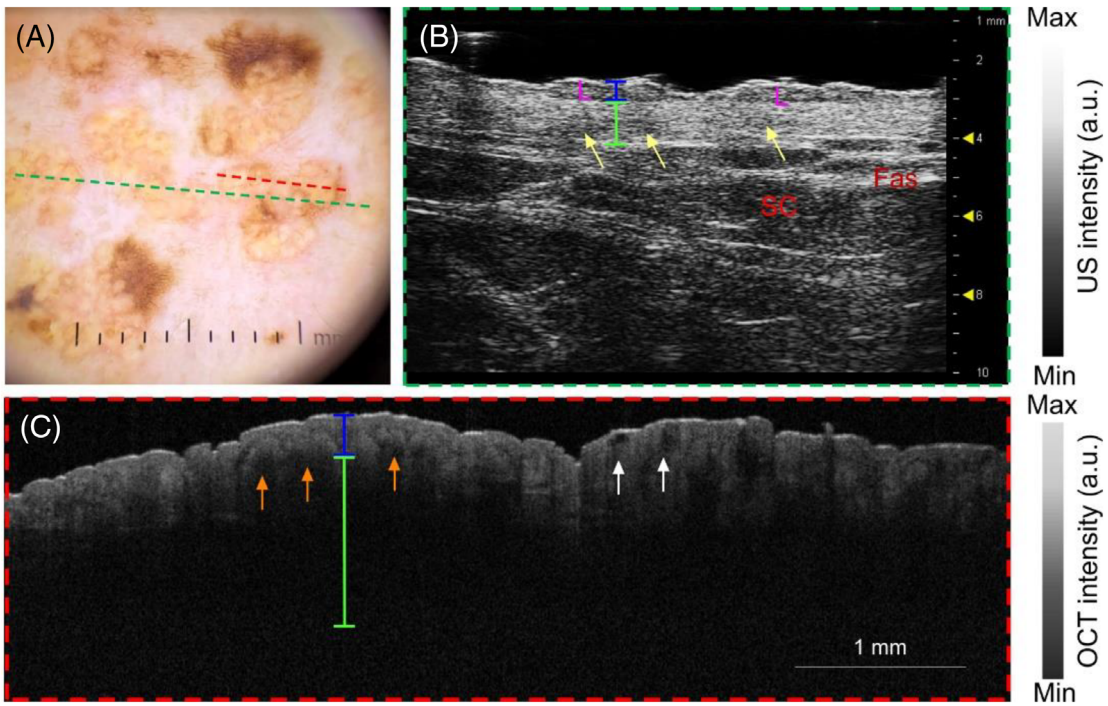

FIGURE 8 Nevus sebaceous (NS) of phacomatosis pigmentokeratotica (PPK) on the chest. **(A)** Dermoscopy image of NS. Yellow-tan globules aggregated in clusters on a lentiginous background with scattered junctional nevi are present. Red dashed line—optical coherence tomography (OCT) probe field (6 mm). Green dashed line—high-frequency ultrasound (HFUS) probe field 16 mm. **(B)** HFUS image of the NS. L—lesion. Blue line—epidermal entry echo. Green line—dermis. Yellow arrows—sebaceous gland hyperplasia. SC—subcutis. Fas—fascia. **(C)** OCT image of the NS. Blue line—epidermis. Green line—dermis. White arrows—papillomatosis. Yellow arrows—papillary dermal collagen deposition. Epidermis is thickened, acanthotic, and hyperkeratotic.

is unable to be visualized on OCT due to the inherent hypoechoic nature and limited light penetration. A summary of HFUS and OCT characteristics of each lesion may be found in Table A1.

4 | DISCUSSION

In this study, we compared dermoscopy, HFUS, and OCT images of benign nevi on an adult patient with PPK with the goal of discerning whether visualizing noninvasive biomarkers demonstrated on imaging may be sufficient to forego biopsy. We successfully correlated imaging patterns seen on noninvasive imaging to histological features outlined in the literature. Dermoscopy provided the most superficial and visual characteristics of a lesion. HFUS allowed for visualization beyond the dermis, providing data on potential depth of invasion of a pigmented lesion. OCT allowed for visualization of the lesion at a higher resolution, providing architectural changes within the epidermis and the upper dermis. Pairing all three imaging modalities together allowed for an in depth understanding of a benign nevus in PPK. We determine that dermoscopy, HFUS, and OCT provide different pieces of data of a lesion, though none are definitive or conclusive independently. When comparing all imaging modalities together, we may piece together multilayered data about the lesion of interest to provide a clearer picture of the whole lesion in a noninvasive manner.

We investigated numerous types of lesions that may be found in a patient with PPK including compound Spitz nevus, compound dysplastic nevus, junctional nevus, and nevus sebaceous. Hyperechoic or bright signal intensities on both HFUS and OCT imaging may reflect structures such as collagen bundles and deposition, keratin distribution, melanin, and acanthosis. Hypoechoic or echo-poor structures include blood vessels, sebaceous glands, apocrine glands, fat, and hair follicles.[27,32] All compound nevi had a consistent pattern on HFUS demonstrating bulging of the hypoechoic lesion extending into the dermis at varying degrees. The hypoechoic lesions imaged in our study demonstrated heterogeneity with small hyperechoic spots within, potentially suggesting areas of melanin accumulation.[18] On OCT images, compound nevi have distinct features of elongated rete ridges with extension into the papillary dermis with occasional rete ridge fusion and rectification. In deeply pigmented lesions such as the nevi on the chest (Figure 4C) and shoulder (Figure 5C), there is a loss of the DEJ signal intensity, with incurring homogenous blending of the epidermis into the dermis.

We further visualized features of subcategories of compound nevi including Spitz and dysplastic. Compound Spitz nevi may have worrisome histological features similar to malignant melanoma. However, additional structures including kamino bodies and pagetoid melanocytic spread indicate the benign nature of the lesion.[22] Due to these, when implementing higher resolution OCT imaging, the entirety of the lesion should be imaged and analyzed to ensure these benign features may be found. Because kamino bodies comprise of type IV and VII collagen, laminin, and fibronectin, these structures would show up as hyperechoic signals in the epidermis on imaging.[36] Cutaneous melanoma on HFUS is described as well-demarcated, homogenous, and hypoechoic, often more so than benign nevi.[32,37] In our study, on HFUS, the compound Spitz nevus of the leg (Figure 7B) blended well into the dermis with increased focal dermal density, uniquely differentiating this lesion from typical HFUS images of melanoma in the literature.[38] Compound dysplastic nevi have unique identifying histological features including lamellar fibroplasia, rete ridge fusion, and shouldering, or the extension of at least three rete ridges beyond lateral margins of the dermis.[24] Cutaneous melanoma on OCT demonstrates greater architectural disorganization with obscure DEJ borders, thickened epidermis, and larger rete ridges.[39] When distinguishing melanoma from compound nevi on OCT, melanoma has a distinct presence of dermal shadows and an absence of bright collagen.[34] With OCT's ability to show architectural changes, we were able to visualize compound nevi rete ridge definition, a well-demarcated DEJ, and the presence of brightly reflective collagen without biopsy. Most importantly, proper melanocytic maturation with more superficial nest proliferation transforming into single file melanocytes with descent into the dermis, defines a benign nevus from melanoma.[19,20] However, both HFUS and OCT are limited in visualizing cellular atypia; therefore, histological examination proves to be useful in this case.

Since junctional nevi do not penetrate the dermis, visualization of these lesions was more challenging. On HFUS, we have observed the hypoechoic strip sign, which correlates well with the literature on discerning junctional nevi from other benign nevi subtypes.[18] The thin nature of junctional nevi on HFUS may be related to the restricted melanocytic proliferations at the DEJ. On OCT, patchy areas of elongated rete ridges were present; however, compared to compound nevi, they were less pronounced.

Due to the potential of nevus sebaceous transforming into benign or malignant neoplasms, astute surveillance is of importance. We examined an area of nevus sebaceous that remained unchanged through the course of patient's life. On HFUS, areas of epidermal thickening and undulation indicate acanthosis.[35] The hypoechoic lesions were well demarcated from the dermis below. The OCT image demonstrated higher resolution view of epidermal acanthosis. There was a lack of DEJ signal intensity, as well as a lack of a definitive dermis layer. Papillomatosis was also observed with the upward projection of dermal papillae to the surface of the skin, causing irregular bumpy patterns in the epidermis.[40] In our imaging study, papillomatosis may be seen with hypoechoic finger-like projections extending toward the surface. Sebaceous gland hyperplasia hypoechogenieity was seen on HFUS imaging, but not in OCT imaging, due to the limited light penetration depth. Since HFUS and OCT differ in imaging depth and resolution, implementing both HFUS and OCT for nevus sebaceous may play a role in observing changes in these lesions over time.

The advantages of HFUS and OCT are its noninvasive character, mobility of the machine, and ability to repeat examination if necessary. HFUS can display the size, shape, and depth of the lesion. Additionally it has been reported that HFUS skin lesion measurements have a high correlation with histopathological data.[35] OCT can demonstrate notable patterns of tissue pathological architecture. In pigmented lesions, these include presence of elongated rete ridges, rete ridge fusion due to melanocytic proliferation, loss of the DEJ signal intensity,

and homogenous blending of the epidermis to the dermis. In nevus sebaceous, epidermal thickening, collagen and keratin accumulation, and papillomatosis may be visualized on OCT. Limitations of HFUS and OCT include a lack of uniformity of examination standards. Image acquisition and quality are dependent on the individual, which may require additional training. HFUS specifically lacks functional contrast, which implies decreased efficacy in differentiating hypoechoic tissues including tumor, fat, and inflammatory infiltrates.[30,31] Its limited resolution prevents visualization at the cellular level, making it difficult to differentiate specific morphology. Additionally, HFUS has a low specificity and inability to diagnose tumor type.[39] Of note, HFUS and OCT imaging results may be dependent on how much perpendicular pressure the user applies to the handheld probe. Increased pressure on the skin may flatten the most superficial parts of the skin such as the epidermis, leading to a perceived thinner epidermis and even a deeper visualization of the fascia and subcutaneous tissue. Alternatively, a lighter probe pressure will help to retain the natural thickness of the epidermis but will have a decreased depth of visualization. HFUS imaging is also dependent on how much space is between the probe and the surface of the skin, which alters the window depth of HFUS images. Because we focus on the structures within the epidermis and dermis, visualization of the fascia and subcutaneous tissue does not affect our data. Additionally, different areas of the body have different thicknesses of the epidermis. A thinner epidermis, such as the face, will have a perceived deeper visualization of the fascia and subcutaneous tissue below the dermis. A thicker epidermis, such as the back, will take more visual space in the HFUS imaging window, leading to a perceived difference in depth of tissue beneath the dermis. Finally, OCT limitations include the inability to distinguish individual cells, light signal intensity decay, anatomical structures causing shadow and light artifact, tissue or OCT probe motion.[41]

5 | CONCLUSION

Biopsy and excision remain the gold standard when assessing and diagnosing suspicious pigmented lesions. However, it is not feasible to remove every skin lesion, especially in cases of clinically diagnosed multiple benign and atypical nevi, exemplified in the PPK case that was presented. This case report demonstrates that implementing additional noninvasive imaging procedures aid in understanding the benign nevi depth, lateral extension, and architectural changes below the surface of the skin. Our current findings and additional unpublished research data demonstrate that noninvasive imaging may increase diagnostic accuracy of benign nevi and aid in initial management or long-term surveillance of the lesion, thus improving patient management. HFUS and OCT features can discern both compound and junctional nevi; however, even with the combination of the two, in conjunction with dermoscopy, there is still a lack of clear cellular differentiation needed to diagnose benign from malignant. We believe this multimodality approach can be a powerful tool during the examination of junctional and more lentiginous nevi and may prevent unnecessary biopsies. Because compound nevi demonstrate greater homogeneity between the epidermis and dermis on imaging, a method with higher clarification of cellular differentiation or optical properties would improve this multimodality approach when preventing biopsies for these lesions. This study demonstrates the increased utility of understanding noninvasive histological patterns and biomarkers of benign nevi involved in a PPK case. Additional imaging studies of benign nevi and larger sample sizes of cases of PPK must be analyzed to substantiate different pattern findings in noninvasive imaging of benign nevi, including those with some architectural disorder and mild to moderate atypia. Qualitative analysis of these lesion's noninvasive biomarkers as well as quantitative analysis of optical properties of the tissue may further increase HFUS and OCT diagnostic capabilities. Quantitative analysis involving the study of attenuation coefficients may prove to be useful in this study. Doing so may be able to compare HFUS and OCT data numerically. The current noninvasive techniques may be useful adjunct tools to clinical examination and dermoscopy in order to define if a biopsy is required in superficial nevi surveillance.

AUTHOR CONTRIBUTIONS

J.L. performed the research, analyzed the data, and wrote the paper. J.L. and K.A. designed the research study. R.M. assisted with preparing figures and reviewed the paper. J.B. and J.M. assisted with imaging procedures. C.P. and J.M. assisted with IRB. M.T. and K.A. assisted financially and reviewed the paper.

ACKNOWLEDGMENTS

Thank you to Dr. Jiwang Chen for his area of expertise in ultrasound imaging. The authors would also like to thank the Melanoma Research Alliance (grant number 624320) for their support.

CONFLICT Of INTEREST

Authors do not report any financial or personal links to other persons or organizations.

DATA AVAILABILITY STATEMENT

Data presented in the article can be provided upon reasonable request.

ORCID

Julia May https://orcid.org/0000-0003-4652-6385

REFERENCES

1. Happle R, Hoffmann R, Restano L, Caputo R, Tadini G. Phacomatosis pigmentokeratotica: a melanocytic-epidermal twin nevus syndrome. *Am J Med Genet*. 1996;65(4):363-5.
2. Baigrie D, Troxell T, Cook C. Nevus Sebaceous. In: *StatPearls [Internet]*. StatPearls Publishing; 2020.
3. Schaffer JV, Orlow SJ, Lazova R, Bolognia JL. Speckled lentiginous nevus: within the spectrum of congenital melanocytic nevi. *Arch Dermatol*. 2001;137(2):172-8.
4. Happle RJ. The group of epidermal nevus syndromes: Part I. Well defined phenotypes. *J Am Acad Dermatol*. 2010;63(1):1-22.
5. Kinsler VA. Melanocytic naevi. 2019;176(5):1237-59.
6. Martínez-Menchón T, Mahiques Santos L, Vilata Corell J, Febrer Bosch I, Fortea Baixauli JM. Phacomatosis pigmentokeratotica: a 20-year follow-up with malignant degeneration of both nevus components. *Pediatr Dermatol*. 2005;22(1):44-7.

7. Medina González AC, Farmer W, Zinn Z, Burgin S. Phakomatosis pigmentokeratotica. 2020. Accessed 12/10/2022. https://www.visualdx.com/visualdx/diagnosis/phakomatosis+pigmentokeratotica?diagnosisId=56631&moduleId=101
8. Groesser L, Herschberger E, Ruetten A, et al. Postzygotic HRAS and KRAS mutations cause nevus sebaceous and Schimmelpenning syndrome. *Nat Genet*. 2012;44(7):783-7.
9. Wollenberg A, Butnaru C, Oppel TJ. Phacomatosis pigmentokeratotica (Happle) in a 23-year-old man. *Acta Derm Venereol*. 2002;82(1).
10. Tadini G, Restano L, Gonzáles-Pérez R, et al. Phacomatosis pigmentokeratotica: report of new cases and further delineation of the syndrome. *Arch Dermatol*. 1998;134(3):333-7.
11. Moody MN, Landau JM, Goldberg LH. Nevus sebaceous revisited. *Pediatr Dermatol*. 2012;29(1):15-23.
12. Vujevich JJ, Mancini AJ. The epidermal nevus syndromes: multisystem disorders. *J Am Acad Dermatol*. 2004;50(6):957-61.
13. Loh S-H, Lew B-L, Sim W-Y. A case of phacomatosis pigmentokeratotica associated with multiple basal cell carcinomas. *Am J Dermatopathol*. 2018;40(2):131-5.
14. Chantorn R, Shwayder T. Phacomatosis pigmentokeratotica: a further case without extracutaneous anomalies and review of the condition. *Pediatr Dermatol*. 2011;28(6):715-9.
15. Groesser L, Herschberger E, Sagrera A, et al. Phacomatosis pigmentokeratotica is caused by a postzygotic HRAS mutation in a multipotent progenitor cell. *Invest Dermatol*. 2013;133(8):1998-2003.
16. Kim YY, Kim MY, Kim TY. Development of halo nevus around nevus spilus as a central nevus, and the concurrent vitiligo. *Ann Dermatol*. 2008;20(4):237-9.
17. Vidaurri-de la Cruz H, Happle R. Two distinct types of speckled lentiginous nevi characterized by macular versus papular speckles. *Dermatology*. 2006;212(1):53-8.
18. Wang YK, Gao YJ, Liu J, et al. A comparative study of melanocytic nevi classification with dermoscopy and high-frequency ultrasound. *Skin Res Technol*. 2021;28(2):265-73.
19. Smolle J, Soyer H-P, Juettner F-M, Hoedl S, Kerl H, Practice. Nuclear parameters in the superficial and deep portion of melanocytic lesions: a morphometrical investigation. *Pathol Res Pract*. 1988;183(3):266-70.
20. Balu M, Kelly KM, Zachary CB, et al. Distinguishing between benign and malignant melanocytic nevi by in vivo multiphoton microscopy. *Cancer Res*. 2014;74(10):2688-97.
21. Mooi WJ. Histopathology of Spitz naevi and "Spitzoid" melanomas. *Dermatopathology*. 2001;94:65-77.
22. Crotty KA, Scolyer RA, Li LXL, Palmer AA, Wang L, McCarthy SW. Spitz naevus versus Spitzoid melanoma: when and how can they be distinguished? *Pathology*. 2002;34(1):6-12.
23. Clemente C, Cochran AJ, Elder DE, et al. Histopathologic diagnosis of dysplastic nevi: concordance among pathologists convened by the World Health Organization Melanoma Programme. *Hum Pathol*. 1991;22(4):313-9.
24. Toussaint S, Kamino H. Dysplastic changes in different types of melanocytic nevi. A unifying concept. *J Cutan Pathol*. 1999;26(2):84-90.
25. Karia DR, Solanki AN, Jagati AG, Shah BJ. Phacomatosis pigmentokeratotica: a very rare twin spotting phenomenon. *J Dermatol Venereol Leprol*. 2018;84(1):120.
26. Rallan D, Bush NL, Bamber JC, Harland CC. Quantitative discrimination of pigmented lesions using three-dimensional high-resolution ultrasound reflex transmission imaging. *J Invest Dermatol*. 2007;127(1):189-95.
27. Mlosek RK, Malinowska S. Ultrasound image of the skin, apparatus and imaging basics. *J Ultrason*. 2013;13(53):212.
28. Hinz T, Ehler L-K, Voth H, et al. Assessment of tumor thickness in melanocytic skin lesions: comparison of optical coherence tomography, 20-MHz ultrasound and histopathology. *Dermatology*. 2011;223(2):161-8.
29. Vidal D, Ruiz-Villaverde R, Alfageme F, et al. Use of high frequency ultrasonography in dermatology departments in Spain. *Dermatol Online J*. 2016;22(2).
30. Schneider SL, Kohli I, Hamzavi IH, Council ML, Rossi AM, Ozog DM. Emerging imaging technologies in dermatology: part I: basic principles. *J Am Acad Dermatol*. 2019;80(4):1114-20.
31. Schneider SL, Kohli I, Hamzavi IH, Council ML, Rossi AM, Ozog DM. Emerging imaging technologies in dermatology: part II: applications and limitations. *J Am Acad Dermatol*. 2019;80(4):1121-31.
32. Harland C, Bamber J, Gusterson B, Mortimer PS. High frequency, high resolution B-scan ultrasound in the assessment of skin tumours. *Br J Dermatol*. 1993;128(5):525-32.
33. Levy J, Barrett DL, Harris N, Jeong JJ, Yang X, Chen SC. High-frequency ultrasound in clinical dermatology: a review. *Ultrasound J*. 2021;13(1):1-12.
34. Blumetti TCMP, Cohen MP, Gomes EE, et al. Optical coherence tomography (OCT) features of nevi and melanomas and their association with intraepidermal or dermal involvement: a pilot study. *J Am Acad Dermatol*. 2015;73(2):315-7.
35. Bezugly A, Sedova T, Belkov P, Enikeev D, Voloshin RJM, Reports P. Nevus sebaceus of Jadassohn-high frequency ultrasound imaging and videodermoscopy examination. Case presentation. *Med Pharm Rep*. 2021;94(1):112.
36. Venkatesh D, Smitha T, Jomfp MP. Kamino bodies. *J Oral Maxillofac Pathol*. 2019;23(1):17.
37. Machet L, Samimi M, Georgesco G, et al. High resolution ultrasound imaging of melanocytic and other pigmented lesions of the skin. *Ultrasound Imaging*. 2011:139-50.
38. Chaput L, Laurent E, Pare A, et al. One-step surgical removal of cutaneous melanoma with surgical margins based on preoperative ultrasound measurement of the thickness of the melanoma. *Eur J Dermatol*. 2018;28(2):202-8.
39. Kratkiewicz K, Manwar R, Rajabi-Estarabadi A, et al. Photoacoustic/ultrasound/optical coherence tomography evaluation of melanoma lesion and healthy skin in a swine model. *Sensors (Basel)*. 2019;19(12):2815.
40. Waltz KM, Helm KF, Billingsley EM. The spectrum of epidermal nevi: a case of verrucous epidermal nevus contiguous with nevus sebaceus. *Pediatr Dermatol*. 1999;16(3):211-3.
41. Adabi S, Turani Z, Fatemizadeh E, Clayton A, Nasiriavanaki M. Optical coherence tomography technology and quality improvement methods for optical coherence tomography images of skin: a short review. *Biomed Eng Comput Biol*. 2017;8:1179597217713475.

How to cite this article: Lee J, Benavides J, Manwar R, et al. Noninvasive imaging exploration of phacomatosis pigmentokeratotica using high-frequency ultrasound and optical coherence tomography: Can biopsy of PPK patients be avoided?. *Skin Res Technol*. 2023;29:e13279. https://doi.org/10.1111/srt.13279

APPENDIX

TABLE A1 Characteristics of different lesions in phacomatosis pigmentokeratotica in high-frequency ultrasound versus optical coherence tomography

Type of lesion	High-frequency ultrasound	OCT
Junctional nevus	Epidermis - "Strip-shaped" hypoechoic signal	Epidermis - Hyperechoic Rete ridge pattern - Elongated - Lentiginous pattern Dermal-epidermal junction - Undulating and nonuniform
Compound nevus	Dermis - Focal hypoechoic signal - "Straw hat sign" - Hyperechoic inferior collagen deposition surrounding nevus	Epidermis - Hyperechoic Rete ridge pattern - Fusion - Broadened - Elongated Dermal-epidermal junction - Undulating and nonuniform
Compound dysplastic nevus	Dermis - Focal hypoechoic signal - "Straw hat sign"	Epidermis - Hyperechoic intensity Rete ridge patterns - Fusion - Broadened - Elongated Dermal-epidermal junction - Undulating and nonuniform Dermis - Hyperechoic signal intensities throughout papillary dermis
Compound Spitz nevus	Epidermis - Thickened hyperechoic epidermal entry echo Dermis - Hypoechoic ovoid signal	Epidermis - Hyperechoic intensity Rete ridge patterns - Fusion - Broadened - Elongated Dermal-epidermal junction - Undulating and nonuniform
Nevus sebaceous	Epidermis - Thickened hyperechoic epidermal entry echo - Connected hypoechoic globules Dermis - Hypoechoic shadows below epidermal hypoechoic globules	Epidermis - Thickened - Homogenous signal intensity blending into dermis Dermis - Flame-shaped hyperechoic signals extending toward epidermis - Hypoechoic oval signals reaching the surface of the epidermis